Contents lists available at ScienceDirect

Biochemistry and Biophysics Reports

Producing amyloid fibrils in vitro: A tool for studying AL amyloidosis

Daria V. Sizova [*], Steve Raiker, Deaneira Lakheram, Vishwanatha Rao, Andrew Proffitt, Yazen Jmeian, Walter Voegtli, Melissa Batonick

Alexion AstraZeneca Rare Disease, 100 College Street, New Haven, CT, 06510, USA

ARTICLE INFO

ABSTRACT

Amyloid light-chain (AL) amyloidosis is the second most common form of systemic amyloidosis which is characterized by a high level of mortality and no effective treatment to remove fibril deposition. This disorder is caused by malfunctioning of B-cells resulting in production of abnormal protein fibrils composed of immunoglobulin light chain fragments that tend to deposit on various organs and tissues. AL amyloidosis is set apart from other forms of amyloidosis in that no specific sequences have been identified in the immunoglobulin light chains that are amyloid fibril formation causative and patient specific. This unusual feature hinders the therapeutic progress and requires either direct access to patient samples (which is not always possible) or a source of in vitro produced fibrils. While isolated reports of successful AL amyloid fibril formation from various patient-specific protein sequences can be found in literature, no systematic research on this topic was performed since 1999.

In the present study we have developed a generalized approach to in vitro fibril production from various types of previously reported [1-3] amyloidogenic immunoglobulin light chains and their fragments. We describe the procedure from selection and generation of starting material, through finding of optimal assay conditions, to applying a panel of methods to confirm successful fibril formation. Procedure details are discussed in the light of the most recent findings and theories on amyloid fibril formation. The reported protocol produces high quality AL amyloid fibrils that can subsequently be used in the development of the much-needed amyloid-targeting diagnostic and therapeutic approaches.

1. Introduction

Monoclonal immunoglobulin light chain amyloidosis, also known as amyloid light-chain amyloidosis or AL amyloidosis, is a disease caused by conversion of excessive immunoglobulin light chains from soluble state into highly organized amyloid fibrillar aggregates that deposit on various organs leading to their dysfunction and ultimate failure. AL amyloidosis predominantly affects heart and kidney, and the extent of cardiac damage is the major determinant of patient survival. The incidence of AL amyloidosis is averaging at 9 cases per million people per year [4] placing this disorder in a rare disease cohort. AL amyloidosis prevalence is increasing with age and doubles in individuals over 65 years old compared to 35–54 years old ones, and 55% of patients are men. In the US alone, there are at least 12,000 adults living with AL amyloidosis and this number is expected to rise over the next decade [5].

Despite recent progress achieved in understanding AL amyloidosis underlying pathology and mechanisms of amyloid fibril formation, less than one-quarter of patients survive for more than 10 years after diagnosis [6]. Current approved therapeutic approaches target the B cell clone responsible for aberrant immunoglobulin light chain (LC) overproduction while the development of novel therapeutics recently started to focus on targeting the pre-amyloid fibril-like formations as well as organ deposited amyloid fibrils [7]. While the diverse nature of antibody sequences found in amyloids from different patients was known for more than half a century [8], the need for a unified approach to generate such fibrils in vitro became clear only recently, with a surge in development of novel amyloid-targeting diagnostic and therapeutic approaches. In the present study we systematically tested various amyloid fibril formation starting materials, assay conditions, and fibril formation confirmatory tests in order to develop a generalized amyloid fibril formation procedure.

---

2. Materials and Methods

2.1. Protein expression and purification

Sequences of all peptides and proteins used in the present study are shown in Table 1. Short peptides were obtained by direct synthesis at New England Peptide (Gardner, MA) with >90% purity by HPLC and MS analysis. Various human VL and VL-CL proteins were recombinantly expressed in mammalian cell systems. A 6x His-tag was cloned to the C-terminus of the coding region of VL or VL-CL protein in a pcDNA 3.1 vector with a secretion signal in the beginning of the recombinant protein. Expi-CHO cells were transfected with the DNA plasmids using ExpiFectamine™ (Thermo) reagent by following manufacturers recommendation. Secreted proteins were collected either in a 5-day at 37 °C growth period (VL-CL proteins) or in a period of 37 °C for 16 h, followed by 11 days at 32 °C in Dynamis media (VL proteins), spun down to pellet cells and filtered through 0.2 μm filters to remove aggregated material.

His-tagged protein purification was done using IMAC protocols using HisTrap HP columns (Cytiva) connected to an AKTA system using a linear gradient of 0–250 mM Imidazole in 20 mM sodium phosphate buffer with 500 mM NaCl, pH7.4. Purified protein was used after dialyzing it against 1xPBS with three changes. Purified proteins were characterized by running on SDS-PAGE under non-reducing (375 mM Tris-HCl (pH 6.8), 9% SDS, 50% glycerol, 0.03% bromophenol blue) and reducing (375 mM Tris-HCl (pH 6.8), 9% SDS, 50% glycerol, 9% β-mercaptoethanol, 100 mM DTT, 0.03% bromophenol blue) conditions.

2.2. In vitro fibril formation procedure

Lyophilized amyloidogenic peptides were reconstituted at 1 mg/ml in 10% Dimethylformamide (DMF) in 1xPBS buffer, pH7.4, aliquoted, and stored at −80 °C. Amyloidogenic VL and VL-CL proteins were expressed and purified as described above and stored at 4 °C. Thioflavin T (ThT) stock solution was prepared in water at 1 mM, filtered through 0.22 μm membrane (Sartorius Stedim, Bohemia, NY), aliquoted and stored at −20 °C in the dark.

Immediately before the start of the fibril formation procedure, peptide/protein samples were centrifuged at $16,000 \times g$ at 4C for 10 min and filtered using 0.22 μm membranes (Sartorius Stedim, Bohemia, NY). Fibril formation samples (20 μM of amyloidogenic peptide or protein and 10 μM Thioflavin T (ThT) in PBS, pH7.4) were prepared on ice and then moved to the black polystyrene 96-well plate (Greiner, Monroe, NC) at 200μl/well. All remaining empty wells of the plate were filled with 200 μl PBS, and the plate was sealed with aluminum plate seal (Diversified Biotech, Dedham, MA). All sides and corners of the plate were tightly secured with tape to prevent evaporation and the plate was covered with a black plate lid to reduce photobleaching. All fibril formation assays were performed at least in triplicates. Samples were incubated at 37 °C with shaking on an orbital shaker Incu-Mixer MP (Benchmark Scientific, Sayreville, NJ), at 900 rpm. Fibril formation was monitored by taking regular readings of ThT fluorescence (excitation at 440 nm, emission at 485 nm) and normalizing the resulting values to the ThT fluorescence signal in a corresponding well before the start of the incubation. Fibril formation was assumed as completed when the normalized ThT fluorescence curve was plateauing at a value higher than 4. Plates were briefly centrifuged before every read to collect the condensate from the seal. Plate seal and tape were replaced after each fluorescence read.

2.3. Analysis of experimental kinetic data

All data were analyzed and graphed using Prism software (GraphPad). Fluorescence signal (ex440nm/em485nm) at each time point was normalized to the ThT signal at time 0 and presented as mean ± S.E. The EC_{50} values of each kinetic experiment was obtained by fitting each data

Table 1
Sequence of the amyloid IgG light chains (LCs) and corresponding fragments that were used in the present study.

Protein name	LC type	VL-CL sequence	VL sequence	Peptide sequence
WIL	Lambda 6	NFLLTQPHSV SESPGKTVTI SCTRSSGSIA NNYVHWYQQR PGSSPTTVIF EDDHRPSGVP DRFSGSVDSS SNSASLTISG LKTEDEADYY CQSYDHNNQV FGGGTKLTVL GQPKAAPSVT LFPPSSEELQ ANKATLVCLI SDFYPGAVTV AWKADSSPVK AGVETTTPSK QSNNKYAASS YLSLTPEQWK SHRSYSCQVT HEGSTVEKTV APTECS	110 N-terminal amino acid residues	24 N-terminal amino acid residues
LEN	Kappa 4	DIVMTQSPDS LAVSLGERAT INCKSSQSVL YSSNSKNYLA WYQQKPGQPP KLLIYWASTR ESGVPDRFSG SGSGTDFTLT ISSLQAEDVA VYYCQQYYST PYSFGQGTKL EIKRTVAAPS VFIFPPSDEQ LKSGTASVVC LLNNFYPREA KVQWKVDNAL QSGNSQESVT EQDSKDSTYS LSSTLTLSKA DYEKHKVYAC EVTHQGLSSP VTKSFNRGEC	114 N-terminal amino acid residues	22 N-terminal amino acid residues
AL-09	Kappa 1	DIQMTQSPSS LSASVGDRVT ITCQASQDIN NYLIWYQQKP GQAPKLLIYD ASTLETGVPS RFSGSGSGTE FTFTISSLQP EDLATYHCQQ YDNLPYTFGQ GTKLEIKRTV AAPSVFIFPP SDEQLKSGTA SVVCLLNNFY PREAKVQWKV DNALQSGNSQ ESVTEQDSKD STYSLSSTLT LSKADYEKHK VYACEVTHQG LSSPVTKSFN RGEC	108 N-terminal amino acid residues	24 N-terminal amino acid residues
AL-T05	Lambda 1b	Not tested	QSVLTQPPSV SAAPGQTVTI SCSGSSSNIG NNYVSWYQHL PGTAPKFLIY DNNKRPSGIP DRFSGFKSGT	Not tested

(continued on next page)

Table 1 (*continued*)

Protein name	LC type	VL-CL sequence	VL sequence	Peptide sequence
			SATLGITGLQ TGDEADYYCG TWDSSLSALV FGGGTKLTVL	

set to a sigmoidal function. Statistical significance was determined using either an independent *t*-test (two samples) or one-way ANOVA followed by Tukey's multiple-comparison test (more than two samples) where appropriate. Differences were reported as statistically significant when p-value was less than 0.05. Statistically significant differences were reported as either *, statistical significance with $p < 0.05$, or **, statistical significance with $p < 0.01$, or ***, statistical significance with $p < 0.001$, or ****, statistical significance with $p < 0.0001$. The absence of statistically significant differences was shown as [ns], not significant.

2.4. Confirmatory tests of in vitro produced fibrils

2.4.1. ThT confirmatory test

Once the time required for fibril formation for a particular amyloidogenic protein was determined using the kinetic experimental procedure as described above, larger batches of each fibril type were produced without addition of ThT to the fibril formation mixture. Instead, ThT (10 µM) was added to a sample before and after fibril formation, and ThT fluorescence was read (excitation at 440 nm, emission at 485 nm). If the ratio between ThT signal from the two samples was found to be greater than 4 fold indicating more than 4x fluorescence enhancement in the final sample, the ThT quality control test was judged as passed. Resulting amyloid fibrils were aliquoted and stored frozen at −80 °C until the next confirmatory step.

2.4.2. Dynamic light scattering (DLS) confirmatory test

Comparison between the two samples before and after fibril formation was performed using a dynamic light scattering instrument (Uncle, Unchained Labs, Pleasanton, CA) by following a standard company recommended protocol. Briefly, 9 µl of a filtered and centrifuged sample of a protein at 20 µM in PBS as well as 9 µl of a corresponding freshly thawed in vitro produced fibril sample were added to the Uncle cartridge, the sample unit was assembled and loaded into the instrument. All samples were tested in triplicate. The sizing and polydispersity project was run, and data was analyzed using Uncle Analysis Software. The hydrodynamic radius for all amyloid VL proteins tested was found to be in the range between 1 and 10 nm, while successfully formed fibrils had this value shifted to the over 100 nm range. Observing such a dramatic shift in hydrodynamic radius served as second test for successful fibril formation.

2.5. Electron microscopy

Fibril samples were stored at −80 °C until staining. The grids used were copper 400 mesh coated in a 5–6 nM layer of amorphous carbon, which were glow discharged immediately before use. The staining agent was freshly prepared 0.75% (w/v) uranyl formate in dH2O, titrated to pH 4.5 and sterile filtered. Sample was applied to the grid and allowed to adsorb for 3 min, removed by blotting, and then exposed to stain. The samples were applied un-diluted/at full concentration. Grids were imaged using a ThermoFisher/FEI Tecnai F30 microscope operating at 300 kV and a Gatan Ultrascan 4k x 4k CCD detector. The full-magnification images were taken between −0.5 and −1.5 µM defocus (adjusted manually on the fly to maximize contrast and detail) at various magnification levels. To obtain average length and width of in vitro generated fibrils, measurements were taken from 10 fibrils per one EM image, 3 images per VL fibril type, and the results were reported as

average value ± SD.

3. Results

3.1. Light chain protein expression for in vitro fibril formation

Three different types of the human immunoglobulin light chains (LCs), lambda 6 (λ6), kappa 4 (κ4), and kappa 1 (κ1), were selected to study in vitro amyloid fibril formation. Full light chains (LC, composed of both variable and constant light chain domains VL-CL proteins) as well as shorter fragments derived from these LC (VL proteins as well as even shorter 22-24 N-terminal amino acid residues long peptides) were tested for their ability to form amyloid fibrils in vitro. Later we added a VL fragment of the lambda 1b (λ1b) light chain type to our collection of in vitro made and quality controlled fibrils. The λ6 amyloidogenic protein was generated from cDNA cloned from marrow-derived plasma cells from a patient (WIL) who had AL amyloidosis and renal amyloid deposits [1], the κ4 amyloidogenic LC was derived from urine samples containing Bence-Jones proteins of another AL patient (LEN [2]), while the κ1 and λ1b sequences were found in cardiac amyloidosis deposits that were named AL-09 and AL-T05 respectively [3]. Amino acid sequences of all proteins and peptides used in the present study are shown in Table 1.

Complete amino acid sequences are presented for each of the protein used in the present study. VL and CL fragments are shown in red and blue colors respectively.

Preparation of the starting material for in vitro fibril formation differed significantly between short peptides, VL fragments and full VL-CL light chains. While short peptides were directly synthesized, larger proteins required a different approach. In previous literature reports, amyloidogenic proteins used for in vitro fibril formation were always expressed and purified from bacterial cells [1,9,10]. In the present study we attempted to produce all amyloidogenic proteins in mammalian cells to include posttranslational modification that would occur endogenously. While expression and purification of full amyloidogenic light chains (VL-CL proteins) in mammalian cells did not represent any challenge, we had to work out a different approach to obtain sufficient amounts of the VL fragments.

Several different approaches to produce VL proteins were tested until an optimal protocol was developed. First, we created a set of VL-PCS-CL-6xHis constructs where the PCS (Protease Cleavage Site) was presented by either FLAG, GGS-FLAG, TEV, or CleanCut sequences. This approach failed to produce substantial amounts of the final VL protein product (data not shown). Next, the standard CHO cell culture media was replaced with Dynamis media (ThermoFisher). This approach resulted in modest improvement of the VL protein yield. Finally, in addition to using Dynamis media, a temperature shift (37 °C for 16 h, followed by 11 days at 32 °C) was tested to increase protein production. This final approach resulted in a dramatic increase in the yield of the VL proteins and was used to express VL fragments for all future in vitro fibril formation experiments. A representative picture of post-purification VL and VL-CL protein samples analyzed by SDS-PAGE (non-reducing and reducing conditions) is shown on Fig. 1. Expected sizes are visualized with the VL protein alone represented by a band at ~13kD and the VL-CL protein – at ~24kD. The ~48kD band observed under non-reducing conditions is most probably a dimer as it is not present under reducing conditions.

The in vitro fibril formation protocol developed here, employed a combination of generalized fibril formation protocols, for example [11, 12]. A medium throughput plate-based format was used to process multiple samples simultaneously with a convenience of immediate data collection by a plate reader. A 20 µM concentration of starting material (either full amyloidogenic VL-CL protein, or VL fragment, or short peptide) in 1x phosphate buffered saline (PBS) solution at pH7.4 was used to remain close to physiological conditions. 10 µM of Thioflavin T (ThT) was present in each sample to allow for monitoring of fibril
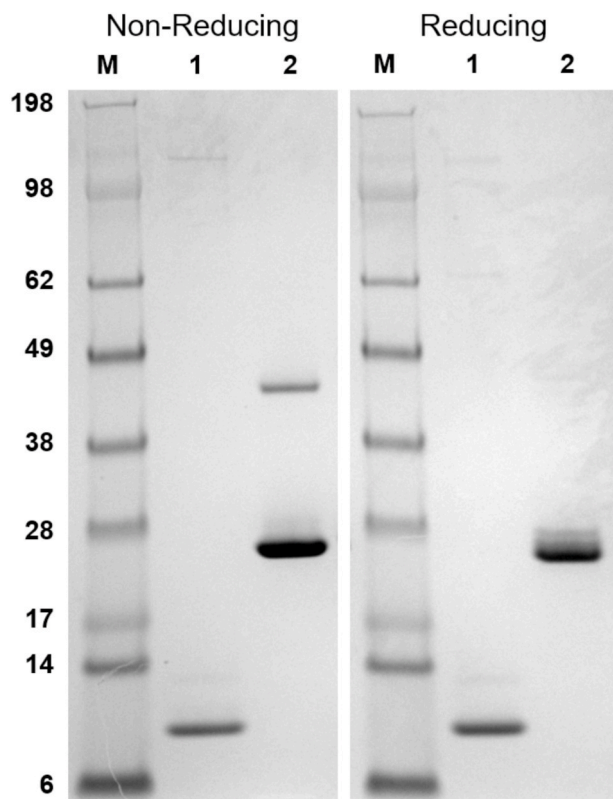
Fig. 1. Representative SDS-PAGE of purified VL and VL-CL proteins.
AL-09 VL (lane 1) and AL-09 VL-CL (lane2) proteins were expressed and puri-fied following an in-house developed procedure (see Materials and Methods for details) and subjected to SDS-PAGE analysis under non-reducing and reducing conditions. Lane M shows a molecular weight marker.

Fig. 2. Kinetics of in vitro fibril formation with amyloidogenic VL proteins.
A, Amyloidogenic VL proteins AL-09 (κ1), LEN (κ4), AL-T05 (λ1b), and WIL (λ6) were subjected to shaking at 37 °C, 900 rpm at 20 μM in PBS, pH7.4 in the presence of 10 μM ThT. Fluorescence signal (ex440nm/em485nm) at each time point was normalized to the ThT signal at time 0 and presented as mean ± S.E. (error bars). Experiments with all four proteins were performed in parallel. **A,** Representative fibril formation kinetic curves of amyloidogenic VL proteins AL-09 (blue circles), LEN (red circles), WIL (green circles), and AL-T05 (purple circle). **B,** Comparison of EC50 values of fibril formation with VL proteins LEN (red column), WIL (green column), and AL-T05 (purple column). *, statistical significance with $p < 0.05$. ****, statistical significance with $p < 0.0001$. The AL-09 VL protein did not produce fibrils under conditions listed above. **C,** Amyloidogenic VL protein AL-09 (κ1) was subjected to fibril formation under standard conditions (37 °C, 900 rpm at 20 μM) except for pH change from 7.4 to 2.0, which resulted in successful fibril formation. The mark of successful fibril formation (normalized ThT signal over 4) is shown on both fibril formation graphs with a dashed black line. (For interpretation of the references to color in this figure legend, the reader is referred to the Web version of this article.)

formation by reading fluorescence at 440 emission/485 excitation wavelengths. The starting solution was centrifuged at $16,000 \times g$, 4 °C for 10 min, and the supernatant was passed through a 0.2 μm filter to remove preformed aggregates. The plate was tightly sealed at the beginning of each kinetic experiment and after each individual fluorescence measurement to prevent evaporation during incubation, and quickly spun down before each fluorescence read to collect the condensate from the plate seal. The plate shaking speed was thoroughly tested and adjusted for the specific type of shaker used (see data below for details) and the temperature was set at 37 °C to mimic physiological conditions. ThT fluorescence was measured regularly, plotted against time, and fibril formation was judged as completed if/when the ThT signal plateaued. As previously suggested, amyloid fibril formation was considered successful when at least 4 fold enhancement in ThT fluorescence was observed compared to time zero [3,10].

3.2. Sequence of the amyloidogenic LC determines the rate of in vitro fibril formation

VL fragments of the full amyloid light chains are known to be prone to fibril formation. To test if fibril formation kinetics differ significantly depending on the sequence of the protein used, we attempted to generate amyloid fibrils from 4 different VL fragments: λ6 WIL, κ4 LEN, κ1 AL-09, and λ1b AL-T05. ThT fluorescence signal (ex440nm/em485nm) at each time point was normalized to the ThT signal at time zero and presented as mean ± S.E. Experiments with all four proteins were performed in parallel. Under standard conditions described above, three out of the four VL proteins successfully formed fibrils with over 4-fold enhancement in ThT fluorescence at plateauing (Fig. 2A and B). The LEN VL protein (kappa light chain type) was found to have the longest
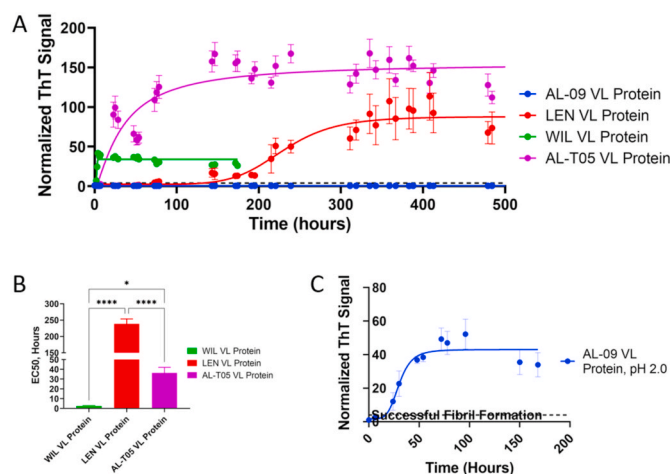
log phase with EC50 of 238.6 ± 15 h; n = 3. This differed significantly ($p < 0.0001$ by one-way ANOVA, followed by Tukey's post hoc analysis) from the other two VL proteins tested (lambda light chain type) that consistently produced fibrils much faster. The EC50 of fibril formation for WIL VL protein was found to be 2.6 ± 0.2 h, n = 4, while it was 36.4 ± 5.6 h, n = 4 for AL-T05 protein. The difference between EC50 values of WIL VL and AL-T05 VL proteins fibril.

Formation (lambda 6 and lambda 1b LC types respectively) was significant as well with $p < 0.05$, by one-way ANOVA followed by Tukey's post hoc analysis. The fourth VL protein tested in this experiment (AL-09, kappa light chain type) did not produce fibrils under standard assay conditions suggesting the need for an adjustment of fibril formation assay variables. Once the pH was lowered from 7.4 to 2.0 (as it was previously suggested for this particular amyloidogenic sequence [3]), successful fibril formation was achieved for AL-09 VL protein as well, Fig. 2C. The EC50 of AL-09 VL protein fibril formation under these modified conditions was 31.0 ± 5.2 h; n = 3. The reported results suggest that, under standard fibril formation protocol employed, the sequence of each amyloidogenic light chain becomes a leading determinant of the rate of in vitro amyloid fibril formation.

3.3. Length of the amyloidogenic LC determines the rate of in vitro fibril formation

To test the effect of the length of a particular amyloidogenic sequence on in vitro fibril formation, we performed fibril formation with short 22–24 amino acid residue long peptides as well as with corresponding full VL-CL light chains for the WIL, LEN, and AL-09 sequences. Amyloidogenic short peptides and full LC VL-CL proteins AL-09 (κ1), LEN (κ4), and WIL (λ6) were subjected to fibril formation under

standard conditions (37 °C, 900 rpm at 20 μM in PBS, pH7.4) in the presence of 10 μM ThT. Fluorescence signal (ex440nm/em485nm) at each time point was normalized to the ThT signal at time 0 and presented as mean ± S.E, Fig. 3A–C. Experiments with all peptides and proteins were performed in parallel. Two out of three short peptides tested formed fibrils very quickly under conditions described above with EC50 of.

43.6 ± 4.5 h, n = 4 (LEN peptide) and 2.6 ± 0.2 h, n = 4 (AL-09 peptide) while WIL peptide did not form fibrils under employed conditions. In contrast, only one full length light chain out of three tested (WIL VL-CL) showed successful fibril formation with EC50 of 93.7±2 h; n = 3. Significant increase in the time required for fibril formation was observed between short peptide LEN and corresponding LEN VL protein, as well as between WIL VL protein and WIL VL-CL proteins (Fig. 3C), by two-way ANOVA, followed by Tukey's post hoc analysis, p < 0.0001 for both comparisons. These results suggest that not only the sequence of amyloidogenic protein but also its length is substantially changing the

Fig. 3. Kinetics of in vitro fibril formation with amyloidogenic short peptides and VL-CL proteins (full LCs). Amyloidogenic short peptides and full LC VL-CL proteins AL-09 (κ1), LEN (κ4), and WIL (λ6) were subjected to fibril formation under standard conditions (37 °C, 900 rpm at 20 μM in PBS, pH7.4) in the presence of 10 μM ThT. Fluorescence signal (ex440nm/em485nm) at each time point was normalized to the ThT signal at time 0 and presented as mean ± S.E. (error bars). Experiments with all peptides and proteins were performed in parallel. **A,** representative fibril formation kinetic curves of amyloidogenic short peptides AL-09 (blue squares), LEN (red squares), and WIL (green squares). **B,** representative fibril formation kinetic curves of amyloidogenic VL-CL proteins AL-09 (blue triangles), LEN (red triangles), and WIL (green triangles). **C,** Comparison of EC50 values of fibril formation with for short peptides, VL proteins, and VL-CL proteins for the same type of amyloidogenic sequence. ****, statistical significance with p < 0.0001. The mark of successful fibril formation (normalized ThT signal over 4) is shown on both fibril formation graphs with a dashed black line. (For interpretation of the references to color in this figure legend, the reader is referred to the Web version of this article.)

kinetics of in vitro fibril formation.

3.4. Additional factors affecting fibril formation

Concentration of the starting material is another factor that could potentially influence in vitro fibril formation kinetics. Amyloidogenic VL protein WIL was subjected to fibril formation under standard conditions (37 °C, 900 rpm, PBS, pH7.4, 10 μM ThT) at 80 μM, 60 μM, 20 μM, 10 μM, 5 μM, and 1 μM concentrations. Fluorescence signal (ex440nm/em485nm) at each time point was normalized to the ThT signal at time 0 and presented as mean ± S.E. No significant difference in fibril formation EC50 values was observed between the three concentrations shown in Fig. 4A (80 μM (blue column): 45.7 ± 2.0, n = 3; 60 μM (red column): 44.9 ± 2.2, n = 3; 20 μM (green column): 46.38 ± 2.4, n = 3), by one-way ANOVA, followed by Tukey's post hoc analysis.

The 10 μM, 5 μM, and 1 μM concentrations did not result in a fibril formation. These results suggest that changing the starting protein concentration within the 20 μM–80 μM range is not affecting the rate of amyloid fibril formation.

Fibril formation may also be influenced by the type of shaker used and by the shaking speed employed. Different instruments have various orbit diameters that substantially influence the kinetic energy at a specific rotational speed. To test this hypothesis, WIL VL protein was subjected to fibril formation under standard conditions (37 °C, 20 μM of protein in PBS, pH7.4, 10 μM ThT) at 410 rpm, 500 rpm, and 1200 rpm on MP orbital plate shaker (Incu-Mixer MP (Benchmark Scientific, Sayreville, NJ), as well as at speed setting #3 (~300 rpm) of Thermo orbital plate shaker (Thermo Scientific Titer Plate Shaker 4625), Fig. 4B. Significant difference in EC50 values was observed between the 410 rpm shaking speed (155.0 ± 27.3, n = 3) and all other shaking speeds/ shakers tested (MP 500 rpm: 57.5 ± 3.6, n = 3; Thermo setting 3: 24.0 ± 0.7, n = 4), by one-way ANOVA, followed by Tukey's post hoc analysis. The 1200 rpm shaking speed did not result in a fibril formation. These findings emphasize the importance of empirically testing the shaker type/shaking speed combination to achieve the optimal fibril formation conditions.

3.5. Confirmatory tests for the new batch of amyloid fibrils

Amyloidogenic VL proteins WIL (λ6) and AL-T05 (λ1b) were subjected to fibril formation under standard conditions (37 °C, 900 rpm at 20 μM in PBS, pH7.4) and tested by three independent confirmatory tests.

The first confirmatory test was based on ThT fluorescence enhancement. ThT was added to sample aliquots before and after fibril formation, and fluorescence signal was measured at ex440nm/ em485nm wavelengths. Normalized ThT signal before and after fibril formation was presented as mean ± S.E. (standard error), and fibril formation was deemed as successful when the ratio between the two was 4 fold, Fig. 5A. A highly significant difference (p < 0001, by unpaired *t*-test) was observed between ThT fluorescence before and after fibril formation, and this difference was greater than 4 fold for both fibril types tested.

The second confirmatory test employed reflected the change in particle size during transition from VL proteins to the final fibril product. This difference in hydrodynamic radius (R_h) was detected using a dynamic light scattering (DLS) approach. Sample aliquots were subjected to the measurement of R_h before and after fibril formation using s dynamic light scattering instrument (Uncle DLS, Unchained Labs). A clear shift from 1 to 10 nm range to over 1,000 nm range suggested a successful fibril formation, Fig. 5B.

The third confirmatory test adopted was a direct visualization of produced fibrils using electron microscopy. After WIL, AL-T05, and AL-09 fibrils were tested by ThT and DLS methods, they were aliquoted and frozen at −80 °C. Thawed samples were stained with aqueous uranyl format solution, and imaging was performed on carbon coated copper
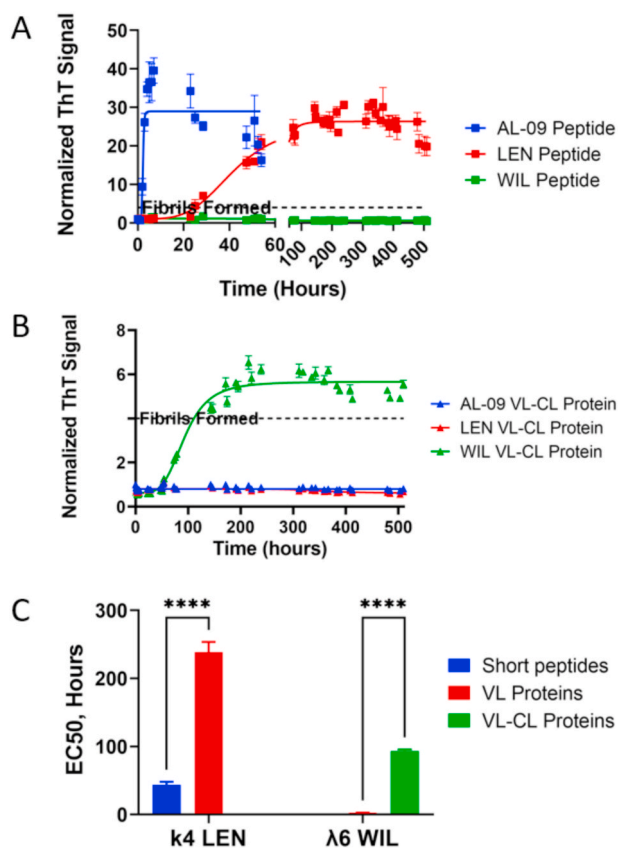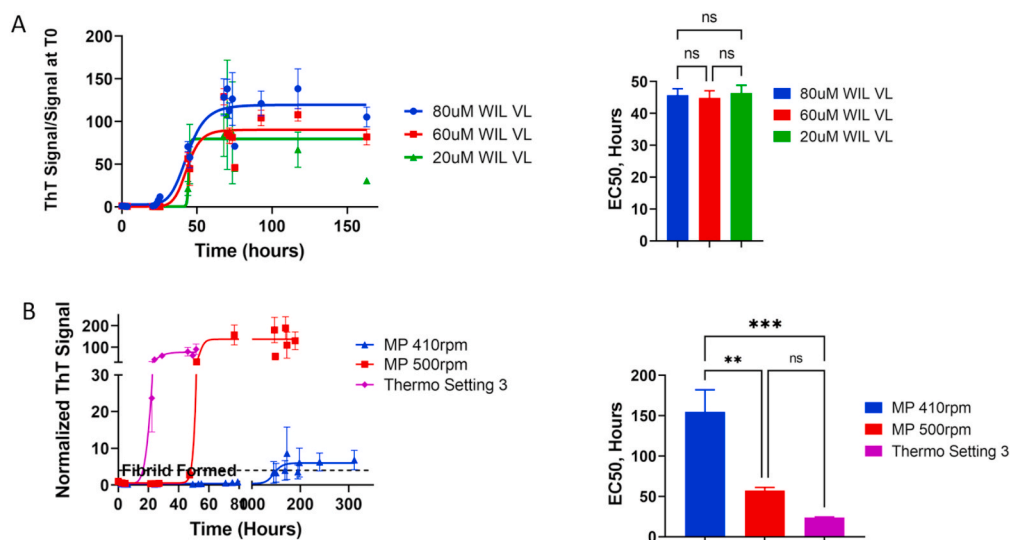
Fig. 4. Additional factors influencing in vitro fibril formation. Amyloidogenic VL protein was subjected to fibril formation under standard conditions (37 °C, 900 rpm at 20 μM in PBS, pH7.4) in the presence of 10 μM ThT. Fluorescence signal (ex440nm/em485nm) at each time point was normalized to the ThT signal at time 0 and presented as mean ± S.E. (error bars). All experiments were performed under the same standard conditions except for one variable changed as indicated for each subfigure. **A,** amyloid fibril formation at different protein concentrations. WIL (λ6) VL protein was subjected to fibril formation at 80 μM (blue circles), 60 μM (red circles), 20 μM (green circles) as well as 10 μM, 5 μM, and 1 μM concentrations (not shown on the graph). **B,** Amyloid fibril formation at different shaking speed/ shaker model. WIL (λ6) VL protein was subjected to fibril formation at 410 rpm (blue triangles), 500 rpm (red squares), and 1200 rpm (not shown on the graph) on MP orbital plate shaker and speed setting #3 of Thermo orbital plate shaker. **, statistical significance with $p < 0.01$. ***, statistical significance with $p < 0.001$. ns, not significant. The mark of successful fibril formation (normalized ThT signal over 4) is shown on both fibril formation graphs with a dashed black line. (For interpretation of the references to color in this figure legend, the reader is referred to the Web version of this article.)
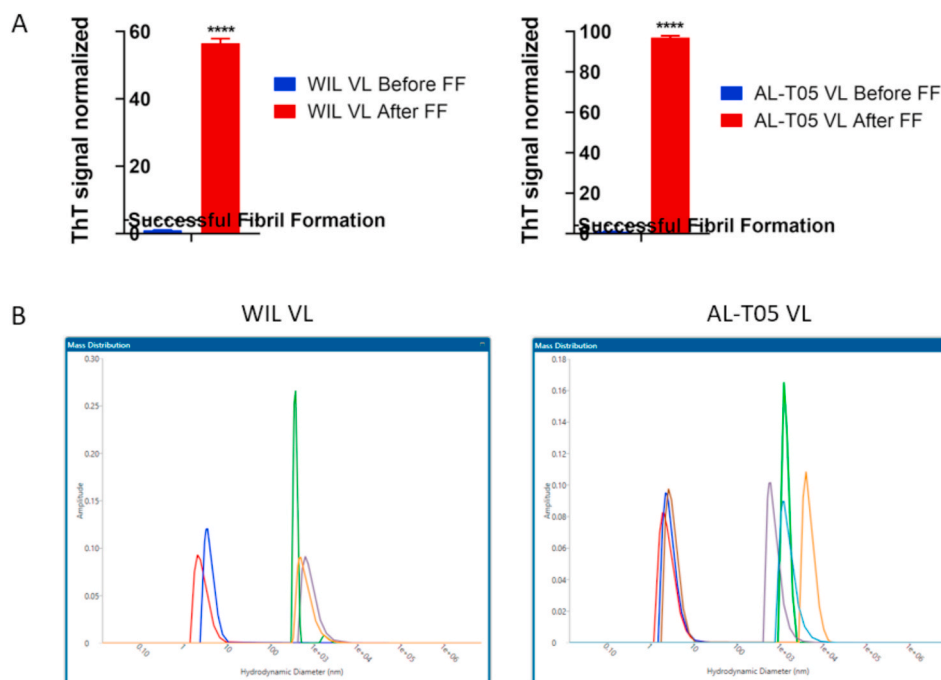

Fig. 5. The use of ThT and DLS-based tests to confirm in vitro fibril formation. Amyloidogenic VL proteins WIL (λ6) and AL-T05 (λ1b) were subjected to fibril formation under standard conditions (37 °C, 900 rpm at 20 μM in PBS, pH7.4). **A,** In vitro produced amyloid fibrils were tested by a ThT-based method. ThT was added to sample aliquots before and after fibril formation, and fluorescence signal was measured at ex440nm/em485nm wavelengths. Normalized ThT signal before and after fibril formation was presented as mean ± S.E. (error bars), and fibril formation was deemed as successful when the ratio between the two was higher than 4 fold. ****, $p < 0001$, by unpaired *t*-test. The mark of successful fibril formation (normalized ThT signal over 4) is shown with a dashed black line. **B,** In vitro produced amyloid fibrils were tested by a DLS-based method. Sample aliquots were subjected to the measurement of hydrodynamic radius before and after fibril formation. A clear shift from 1 to 10 nm range to over 1,000 nm range suggests a successful fibril formation.

mesh grids using a ThermoFisher/FEI Tecnai F30 microscope operating at 300 kV and a Gatan Ultrascan 4k x 4k CCD detector. Images shown on Fig. 6 were taken with nominal magnification factor of either 39000x (left column) or 75000x (right column) with a scale bar (black line in the left bottom corner of each image) representing either 100 nm or 50 nm, respectively. All in vitro generated fibrils have shown a classical AL amyloid fibril morphology [13,14] of rod-like non-branching structures of approximately 10 nm width and varying length. As it is described in the Materials and Methods section, measurements were taken from EM images and resulted in the following values: WIL VL fibrils, 111 ± 39 nm long and 10 ± 3 nm wide, AL-09 VL fibrils, 103 ± 45 nm long, 11±2 nm wide, AL-T05 fibrils, 183 ± 56 nm long, 10 ± 2 nm wide. The electron microscopy visualization provided a direct evidence of successful fibril formation.

4. Discussion

AL amyloidosis is set apart from other types of amyloidosis disorders by the patient-specific uniqueness of the amyloid forming protein. The VJ rearrangement and somatic hypermutation (SHM) can result in VL domains with significantly altered structure [15] suggesting that different LC amino acid sequences can promote fibril formation through
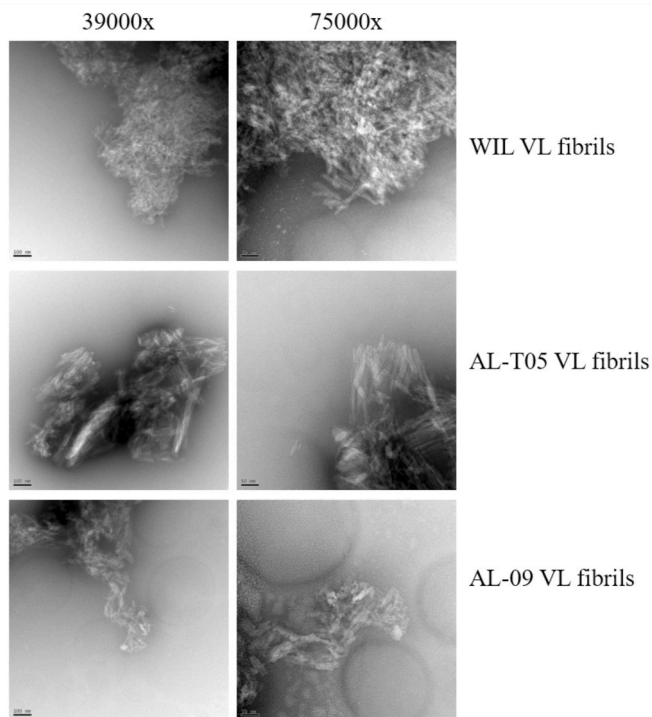
Fig. 6. Representative electron microscopy images of in vitro produced fibrils. Amyloidogenic VL proteins WIL (λ6), AL-09 (κ1), and AL-T05 (λ1b) were subjected to fibril formation under standard conditions (except for pH 2.0 instead of pH 7.4 was used in case of the AL-09 VL protein). Resulting fibrils were tested by ThT and DLS methods, aliquoted and frozen at −80 °C. Thawed samples were stained with aqueous uranyl format solution, and imaging was performed on carbon coated copper mesh grids using a ThermoFisher/FEI Tecnai F30 microscope operating at 300 kV and a Gatan Ultrascan 4k x 4k CCD detector. Images shown were taken at microscope nominal magnification factor of either 39000x (left column) or 75000x (right column) with a scale bar (black line in the left bottom corner of each image) representing either 100 nm or 50 nm, respectively.

somewhat different mechanisms. In addition to the variability resulting from gene segment recombination, light chain somatic mutations arise due to underlying plasma cell dyscrasia thus increasing the patient to patient sequence variability [16]. The amyloid-driving mutation can either destabilize and promote misfolding of the soluble form of the LC by altering its thermodynamic properties or stabilize the fibrillar form by creating additional interactions between the stacked monomers constituting the fibril or have both effects at the same time. In the present study, we used a systematic approach to in vitro fibril formation by testing the propensity to fibrillogenesis of different kappa and lambda amyloid LCs, full VL-CL proteins as well as VL fragments only and corresponding short peptides. As a result, we have developed a procedure that allows the production of amyloid fibrils in vitro independently of the LC type or mutations observed. Considering the large variety of LC sequences found in AL amyloid patient samples, we believe that our protocol represents a useful tool for studying AL amyloidosis, finding better diagnostic approaches, and creating novel amyloid-targeting therapies.

High levels of free light chain monomers and homodimers in patient's body fluids represent one of the main hallmarks of AL amyloidosis. It is also known that the CL domain has a stabilizing effect on the VL domain, and, in the context of AL amyloidosis, in vivo proteolytic cleavage results in the release of the highly fibrinogenic free VL proteins [17]. The so called "VL-model" of AL amyloidosis suggests that in vivo proteolysis is indispensable for amyloid fibril formation and takes place either in the bloodstream before the start of the fibrillation process or in tissue after fibrils are already formed [16]. Various mutations detected

in AL Amyloidosis patient samples appear to decrease the stability of LCs and to promote their partial unfolding that might make the corresponding LCs more accessible for endo-proteolysis. The central core of most amyloid fibrils was shown to be consistent of VL fragments or at least C-terminally truncated LCs [18–20] thus suggesting these fragments to be the main building blocks in corresponding occurrences of AL Amyloidosis. In the present study we were able to generate fibrils from all the amyloidogenic VL sequences tested (while failed to achieve fibril formation with some of the corresponding amyloidogenic peptides and VL-CL proteins) thus confirming that VL fragments should be the first choice of starting material for the in vitro fibril production.

While the VL domain was found to be the main component of amyloid fibrils in many AL amyloidosis studies, some patient samples contain fibrils composed of the full LCs and even CL domains only [16], and the hypothesis that proteolytic cleavage may occur not before but after amyloid fibrils formation is still actively discussed [21]. At the same time, Morgan et al. reported that they were not able to form fibrils in vitro using the full VL-CL protein and suggested that pre-fibril formation proteolytic cleavage and release of the more amyloidogenic VL part is a necessary requirement for successful fibril formation [22]. These contradicting results about the occurrence and timing of LC proteolysis in respect to fibril formation may suggest that this process is a case dependent phenomenon. We have shown successful fibril formation (confirmed by ThT fluorescence only) with only one out of three full amyloid VL-CL proteins under tested conditions which supports this hypothesis. The important role of CL domain in preventing aggregation and the potential of the CL-CL interface as a target for AL Amyloidosis drug development is discussed by Rennella et al. [23].

The short peptides composed of 22–24 N-terminal amino acid residues were previously reported to form fibrils in vitro through agitation-stimulated fibrillogenesis [11]. While this type of starting material is not commonly used for in vitro fibril formation, the accessibility of such reagent through direct synthesis makes it relatively attractive. We have observed successful fibril formation under suggested assay conditions from all short peptides except for one. Despite the significantly reduced time required for fibril formation from short peptides compared to VL proteins (EC_{50} change from days to hours), we do not recommend using this starting material for routine in vitro fibril production because quality control of resulting fibrils represents a challenge. Moreover, the structure of amyloid fibrils formed from short peptides may differ dramatically from patient fibrils thus precluding their use in amyloid-targeting drug development.

The precise mechanism of amyloid fibril formation remains a matter of investigation. A substantial structural reorganization appears to be required for this process to be successful. The native fibrinogenic protein needs to unfold from its natural soluble state to adopt a more energetically favorable amyloid state. Protein unfolding combined with an additional triggers needed to breakdown the supersaturation barrier separating the phase transition from a soluble monomer to a highly ordered amyloid structure. These events are taking place during a rate-limiting lag phase preceding actual amyloid fibril formation and cannot be monitored by ThT which binds to formed fibrils only [24,25]. Subsequent steps of the fibrillation process appear to include formation of non-native dimers that may act as a nucleus for oligomerization to hexamers, then higher oligomers, and finally fibril formation [26].

In AL Amyloidosis, the free LCs are secreted into the blood stream where they are exposed to various proteins, glycosaminoglycans (GAGs), and lipids. All these factors can influence the course of fibril formation, and the resulting effect may be dependent on the nature of patient-specific sequences of those LCs. Polysaccharides, for example, were hypothesized to have the ability to stabilize fibrils by forming salt bridges by binding to accessible basic residues in the fibrils [27], a process that would explain the accelerating effect of GAG that was shown for some amyloid proteins in vitro [10,28–30]. Our study suggests that the presence of additional chaperones or accessory molecules is not mandatory for successful fibril formation in vitro implying that

most of the propensity to fibrillogenesis lies with this amyloid protein itself.

Amyloid fibril formation was previously shown to be an autocatalytic reaction where the presence of homo-fibril or occasionally hetero-fibril "seeds" can significantly accelerate the process [3]. Using elevated temperature is another factor that could increase the speed of fibril formation although resulting fibrils would have a potential to differ significantly from the fibrils formed under physiological conditions. While these approaches may become indispensable to produce fibrils in vitro if the standard protocol proposed in the present study fails, we did not need to use them with the four amyloidogenic VL sequences tested. However, we recommend recurring to this possibility with VL sequences that may be less prone to in vitro fibril formation.

Once the best fibril formation conditions are established for a given amyloidogenic protein, a larger quantity of corresponding fibrils can be produced without addition of 10 μM ThT to the starting mixture. The resulting new batch of fibrils needs to be subjected to several independent quality control methods to confirm the successful fibril production. For the last 20 years the gold standard of amyloid fibrils identification has not changed: the best way to confirm successful fibril formation is (1) - electron microscopy that readily detects the unbranching linear fibrils of variable length and approximately 7–10 nm in diameter closely followed by (2) – either fluorescence enhancement test with thioflavin T (ThT) or birefringence test with Congo red [11]. Electron microscopy, while being the best and ultimate confirmation for successful fibril formation, is not a readily available method, especially in the pharmaceutical research setting. Congo red staining, while largely used for identification of amyloids in ex vivo tissue slices, is less sensitive than ThT in the detection of amyloid fibrils and may also interfere with the aggregation mechanisms [31]. In the present study we have shown that the dynamic light scattering (DLS) approach provides another reliable quality control test for routine in vitro fibril production when used in combination with a ThT fluorescence enhancement test. For best results, we recommend using all three fibril characterization tests (ThT, DLS, and EM) to confirm successful fibril formation for every new amyloidogenic sequence. Subsequently, only two tests (for example, ThT and DLS) should be sufficient to quality control new batches produced following the now established protocol.

At the present moment, it is not possible to tell which one(s) of the mutations that are routinely found in AL patient fibrils are actually disease causing, and it is quite possible that new additional mechanisms for shifting LCs into the amyloid state are yet to be discovered [16]. Until then the progress in AL Amyloidosis research will be dependent on either the availability of patient samples or on the ability to produce patient-specific amyloid fibrils in vitro. We believe that with the detailed generalized in vitro AL amyloid fibril production and confirmatory procedure proposed in the present study, the latter task will become substantially easier thus facilitating future research directed to transforming this deadly disorder into a treatable disease.

Declaration of competing interest

The authors declare that they have no known competing financial interests or personal relationships that could have appeared to influence the work reported in this paper.

References

[1] J. Wall, et al., Thermodynamic instability of human lambda 6 light chains: correlation with fibrillogenicity, Biochemistry 38 (42) (1999) 14101–14108.

[2] A. Solomon, C.L. McLaughlin, Bence-Jones proteins and light chains of immunoglobulins. I. Formation and characterization of amino-terminal (variant) and carboxyl-terminal (constant) halves, J. Biol. Chem. 244 (12) (1969) 3393–3404.

[3] L.M. Blancas-Mejía, M. Ramirez-Alvarado, Recruitment of light chains by homologous and heterologous fibrils shows distinctive kinetic and conformational specificity, Biochemistry 55 (21) (2016) 2967–2978.

[4] M. Zampieri, et al., Incidence of light chain amyloidosis in Florence metropolitan area, Italy: a population-based study, Amyloid 28 (3) (2021) 211–212.

[5] T.P. Quock, et al., Epidemiology of AL amyloidosis: a real-world study using US claims data, Blood Adv 2 (10) (2018) 1046–1053.

[6] G. Merlini, et al., Systemic immunoglobulin light chain amyloidosis, Nat. Rev. Dis. Prim. 4 (1) (2018) 38.

[7] R. Chakraborty, S. Lentzsch, Emerging drugs for the treatment of light chain amyloidosis, Expet Opin. Emerg. Drugs 25 (3) (2020) 299–317.

[8] G. Glenner, et al., Human amyloid protein: diversity and uniformity, Biochem. Biophys. Res. Commun. 41 (4) (1970) 1013–1019.

[9] J.S. Wall, et al., Bifunctional amyloid-reactive peptide promotes binding of antibody 11-1F4 to diverse amyloid types and enhances therapeutic efficacy, Proc. Natl. Acad. Sci. U. S. A. 115 (46) (2018) E10839–e10848.

[10] L.M. Blancas-Mejía, et al., Differential effects on light chain amyloid formation depend on mutations and type of glycosaminoglycans, J. Biol. Chem. 290 (8) (2015) 4953–4965.

[11] J. Wall, C.L. Murphy, A. Solomon, In vitro immunoglobulin light chain fibrillogenesis, Methods Enzymol. 309 (1999) 204–217.

[12] D. Sui, M. Liu, M.H. Kuo, In vitro aggregation assays using hyperphosphorylated tau protein, JoVE (95) (2015), e51537.

[13] G. Merlini, AL amyloidosis: from molecular mechanisms to targeted therapies, Hematology Am Soc Hematol Educ Program 2017 (1) (2017) 1–12.

[14] L. Radamaker, et al., Cryo-EM structure of a light chain-derived amyloid fibril from a patient with systemic AL amyloidosis, Nat. Commun. 10 (1) (2019) 1103.

[15] A.K. Mishra, R.A. Mariuzza, Insights into the structural basis of antibody affinity maturation from next-generation sequencing, Front. Immunol. 9 (2018) 117.

[16] R.M. Absmeier, et al., Antibodies gone bad - the molecular mechanism of light chain amyloidosis, FEBS J. (2022 Feb 4), https://doi.org/10.1111/febs.16390. Online ahead of print.

[17] B. Weber, et al., Domain interactions determine the amyloidogenicity of antibody light chain mutants, J. Mol. Biol. 432 (23) (2020) 6187–6199.

[18] L. Oberti, et al., Concurrent structural and biophysical traits link with immunoglobulin light chains amyloid propensity, Sci. Rep. 7 (1) (2017), 16809.

[19] G.J. Morgan, G.A. Usher, J.W. Kelly, Incomplete refolding of antibody light chains to non-native, protease-sensitive conformations leads to aggregation: a mechanism of amyloidogenesis in patients? Biochemistry 56 (50) (2017) 6597–6614.

[20] F. Lavatelli, et al., Mass spectrometry characterization of light chain fragmentation sites in cardiac AL amyloidosis: insights into the timing of proteolysis, J. Biol. Chem. 295 (49) (2020) 16572–16584.

[21] S. Enqvist, K. Sletten, P. Westermark, Fibril protein fragmentation pattern in systemic AL-amyloidosis, J. Pathol. 219 (4) (2009) 473–480.

[22] G.J. Morgan, J.W. Kelly, The kinetic stability of a full-length antibody light chain dimer determines whether endoproteolysis can release amyloidogenic variable domains, J. Mol. Biol. 428 (21) (2016) 4280–4297.

[23] E. Rennella, et al., Role of domain interactions in the aggregation of full-length immunoglobulin light chains, Proc. Natl. Acad. Sci. U. S. A. 116 (3) (2019) 854–863.

[24] A. Schmidt, et al., Cryo-EM reveals the steric zipper structure of a light chain-derived amyloid fibril, Proc. Natl. Acad. Sci. U. S. A. 113 (22) (2016) 6200–6205.

[25] M. Noji, et al., Breakdown of supersaturation barrier links protein folding to amyloid formation, Commun Biol 4 (1) (2021) 120.

[26] Z. Qin, et al., Structural characterization of the partially folded intermediates of an immunoglobulin light chain leading to amyloid fibrillation and amorphous aggregation, Biochemistry 46 (11) (2007) 3521–3531.

[27] E. Lewkowicz, S. Jayaraman, O. Gursky, Protein amyloid cofactors: charged side-chain arrays meet their match? Trends Biochem. Sci. 46 (8) (2021) 626–629.

[28] F.J. Stevens, R. Kisilevsky, Immunoglobulin light chains, glycosaminoglycans, and amyloid, Cell. Mol. Life Sci. 57 (3) (2000) 441–449.

[29] R. Ren, et al., Role of glycosaminoglycan sulfation in the formation of immunoglobulin light chain amyloid oligomers and fibrils, J. Biol. Chem. 285 (48) (2010) 37672–37682.

[30] R.W. McLaughlin, et al., The effects of sodium sulfate, glycosaminoglycans, and Congo red on the structure, stability, and amyloid formation of an immunoglobulin light-chain protein, Protein Sci. 15 (7) (2006) 1710–1722.

[31] Z.L. Almeida, R.M.M. Brito, Structure and aggregation mechanisms in amyloids, Molecules 25 (5) (2020).